Quaternary International 493 (2018) 176–186

Contents lists available at ScienceDirect

Quaternary International

journal homepage: www.elsevier.com/locate/quaint

Provenance, paleo-weathering and -redox signatures of estuarine sediments from Ghana, Gulf of Guinea

Edem Mahu[a,b], Daniel K. Asiedu[c], Elvis Nyarko[a], Samuel Hulme[b], Kenneth H. Coale[b], Chris Y. Anani[c,*,1]

[a] Department of Marine and Fisheries Sciences, University of Ghana, Ghana
[b] Moss Landing Marine Laboratory, California State University, USA
[c] Department of Earth Science, University of Ghana, Ghana

ARTICLE INFO

Keywords:
Geochemistry
Weathering
Redox conditions
Passive continental margin

ABSTRACT

This paper discriminates the source of sediment supply (provenance), degree of chemical weathering, and redox conditions of Holocene sediments cored from the Ankobra and Pra estuaries of Ghana in the Gulf of Guinea using their geochemical characteristics. Considerable stratigraphical variations were observed in major element compositions in the sediments from both the Ankobra (Al_2O_3: 5.3–14.2%, SiO_2: 75.9–88.2%, CaO: 0.3–1.2%, K_2O: 0.5–1.2%) and the Pra (Al_2O_3: 7.8–16.9%, SiO_2: 72.8–86.5%, CaO: 0.3–0.4%, K_2O: 0.7–1.2%) estuaries. Elemental compositions were similar in both estuaries depicting similarities in their source rock characteristics. Some of the major and trace elements correlated significantly ($r^2 > 0.8$) with Al_2O_3 in the Pra estuary confirming their possible hydraulic fractionation. Geochemical classification showed the sediments from both estuaries were predominantly composed of sub-arkoses with only a few litharenites. The chemical index of alteration (CIA*), Chemical index of weathering (CIW*), plagioclase index of alteration (PIA*), the Index of compositional variability (ICV), the SiO_2/Al_2O_3 ratios and SiO_2 vs. ($Al_2O_3 + K_2O$ + NaO), suggest high degrees of chemical weathering coinciding with warm climatic conditions in the source regions as well as sub-matured to mature estuarine sediments deposited under semi-arid to semi-humid conditions. The sediment geochemistry and discrimination diagrams denote similar continental signature derivatives of the sediments from both estuaries. Both sediments are likely derived from intermediate to felsic granitoid source rocks as well as from a quartzose sedimentary provenance formed in a passive continental margin. The Ni/Co and V/Cr ratios depict sediment deposition under oxic conditions through time in both estuaries.

1. Introduction

Estuaries are productive adjoining coastal systems that serve multiple functions including providing economic, cultural and ecological benefits to communities as well as delivering invaluable ecosystem services to marine and freshwater organisms (Morillo et al., 2008; Burgos and Rainbow, 2001). Despite the important roles played by estuaries across the globe, they have also come under serious threat of pollution, particularly, nutrients and heavy metal pollution mainly due to their geochemical cycling and filtering roles (Ridgway and Shimmield, 2002).

The geochemistry of trace metals and nutrients in estuarine environments is strongly coupled to the source of sediment supply and also the processes controlling their flux into depositional basins such as redox potential and pH (Dobrzinski et al., 2004; Ehrlich, 1996). As sediments are often the ultimate sink for trace metals in estuarine and other aquatic systems, a provenance study on the sediments is relevant for understanding geochemical transformation of trace metals from their source to sink. Provenance, encompasses all factors relating to the production of sediment, with specific reference to the composition of the parent rocks, physiography and climate of the source of the source area from which the sediments are derived (Weltje and von Eynatten, 2004). Provenance studies of nearshore sediments are relevant in nearshore geochemical studies because information gathered from such studies are useful in providing understanding into the main source of sediment supply and to some extent the source potential contaminants that are carried into depositional basins (Singh and Rajamani, 2001).

The geochemical approach to provenance analysis of sediments is based on the effect of chemical weathering on their source materials. Chemical weathering results in the dissolution of primary minerals

* Corresponding author.
E-mail addresses: agbekoen@yahoo.com, cyanani@ug.edu.gh (C.Y. Anani).
[1] Present address: Department of Earth Science, University of Ghana, P.O. Box LG 58, Legon-Ghana.

https://doi.org/10.1016/j.quaint.2018.06.005
Received 13 December 2017; Received in revised form 3 May 2018; Accepted 4 June 2018
Available online 05 June 2018

(particularly feldspars), leading to selective leaching of cations based on the reactivity (Nesbitt and Young, 1996). This results in the concentration of immobile elements and depletion of mobile elements in fluvially-derived sediments (Nesbitt and Young, 1996). Consequently, ratios between mobile and immobile elements change during chemical weathering, as cations have different mobilities in aqueous fluids (Roy et al., 2008). The relative contribution of mobile and immobile ion inputs to nearshore and shelf sediment is the principal factor controlling their bulk chemical composition, giving valuable insights into the mechanisms and processes involved in source rock regions, sediment formation, transport, deposition, hydrodynamic regimes and lithology of the adjacent land areas (Condie, 1993). Estimation of weathering of silicates quantitatively from indices like the chemical index of weathering (CIW), plagioclase index of alteration (PIA) and chemical index of alteration (CIA), are generally employed to deduce the history of weathering of ancient and modern sediments (Roy et al., 2008). As the degree of chemical weathering also depends on climate and rates of tectonic uplift in the source region (Mortazavi et al., 2014), increasing chemical weathering intensity of continental materials may suggest a decrease in tectonic activity and/or a change of climates towards warm and humid conditions (Jacobson et al., 2003).

In the same way, geochemical variables have been adopted by many workers to decipher the paleo-oxygenation condition of ancient sedimentary environments and basins (Cullers, 2002; Dobrzinski et al., 2004). Studies have shown that under varying redox states, trace metals such as Arsenic (As), Mercury (Hg), Chromium (Cr) among others exhibit unique sensitivity to mobilization (Azcue and Nriagu, 1995). For example, the concentration of both As (III) and As (V) in free and pore water is solely a function of the redox potential as the more toxic form, As (III) may dominate under anoxic conditions while As (V) may dominate under oxic condition (Ehrlich, 1996).

As part of national effort to understand the geochemistry of trace elements in the Ankobra and Pra estuaries, this paper seeks to provide further understanding into the heavily polluted nature of the estuaries particularly with As and Hg (Mahu, 2014), by elucidating the source of sediment supply as well as prevailing environmental condition (redox state) at the time of sediment deposition.

2. Geological setting

The geology of Ghana is divided into four tectono-stratigraphic units. These are: (i) Late Paleozoic to Mesozoic sedimentary basins; (ii) mobile belt situated to the east of the West African Craton, and evolved during the Pan-African orogeny (around 600 Ma) also known as the Dahomeyide Belt; (iii) early Proterozoic crystalline rocks collectively known as the Birimian and Tarkwaian rocks and, (iv) Neo-Proterozoic sedimentary cover called the Voltaian Basin (Osae et al., 2006, Fig. 1). The underlying geology of the study areas of both Ankobra and Pra estuaries comprise mainly of early Proterozoic basement rocks called the Birimian Supergroup (Petersson et al., 2018; Leube et al., 1990) (Fig. 1). These early Proterozoic age (Sm-Nd isochron age = 2166 ± 66 Ma) rocks form part of the West African Craton (WAC). They consists of five parallel, evenly spaced, several-hundred-kilometre-long volcanic belts, consisting mainly of low-grade metamorphic, tholeiitic lavas. The belts are separated by basins containing isoclinally folded dacitic volcaniclastics, wackes and argillitic sediments as well as granitoids and are of Paleoproterozoic age (Petersson et al., 2018; Leube et al., 1990). The Birimian lavas and sediments were folded in the course of the Eburnean tectono-thermal event, intruded by various types of granitoids, uplifted and eroded. The erosion products were deposited as sediments of the Tarkwaian Group (Fig. 1) in long, narrow intramontane grabens which formed due to rifting preferentially in the central portions of all five Birimian volcanic belts.

Two major types of Eburnean granitoids in Ghana are characterized as follows: basin granitoids (known as 'Cape Coast type'). They occur as synorogenic foliated batholiths chiefly in the central portions of Birimian sedimentary basins; they are peraluminous and generally granodioritic in composition. Belt granitoids (known as 'Dixcove type'). They mostly form late-orogenic unfoliated intrusions in volcanic belts. They possess a metaluminous character and commonly are of tonalitic composition. Bongo granitoids are of post-Tarkwaian age and K-rich. In contrast to these granitoid types which have strong mantle affinities, the 'Winneba type' had an Archean sialic precursor.

The Ankobra river takes its source in the Kumasi basin (Fig. 1) and generally flows through the same Kumasi basin whiles the Pra river takes its source from the confluence of both Anum and Birim rivers (Fig. 1), all within the Cape Coast basin and continues to flow through the same basin. The lower reaches of both rivers (Ankobra and Pra) commonly drain and establish their estuaries along the fringes of the Ashanti belt (Fig. 1). Both Kumasi basin and Cape coast basins have same intrusive rocks (known as the Cape coast type granitoids) with their associated metasediments (Fig. 1).

3. Materials and methods

Two push sediment cores (one from each estuary) were taken close to the mouths of the Ankobra and Pra estuaries using 60 cm × 8 cm PVC Uwitec corers in 2012. The cores were transported in upright positions to the laboratory where their over lying waters were gently syphoned. Information on each core are presented in Table 1. Each core was sub-sectioned at 2 cm intervals and oven-dried at 60 °C to constant weight. Elemental analysis was carried out at Moss Landing Marine Laboratories (MLML) in California, USA.

Oxides of major elements (SiO_2, Al_2O_3, TiO_2, $Fe_2O_{3(t)}$, CaO, MgO, Na_2O, K_2O, MnO, RbO and P_2O_5) and trace elements (V, Cr, Ni, Co, Rb, and Mn) were measured in digested sediments using a Pelkin-Elmer Element 2 Inductively Coupled Plasma Mass Spectrometry (ICP-MS). Procedure for preparation and digestion of sediments for trace and major elements analysis are reported in Mahu et al. (2015) and Mahu et al. (2016). Grain size analysis was performed on each 2 cm section of the oven-dried sediment using a pre-calibrated Beckman Coulter LS -1320 laser particle sizer at MLML. Ultra-sonication technique was used in disaggregating the sediment where necessary. Sediment fractions in both estuaries were on the average composed of silt (40%) and sand (40%) with clay forming the least fraction. Precision the elemental examination was estimated using the marine sediment reference material BCSS-1 specifications. Metal recoveries differed between 88% and 105% element in each estuary (Table 2). Analytical accuracy determined using six duplicates of a homogenized sample varied from 4% to 6% for major elements and 4%–8% trace elements.

From the geochemical data (Table 3), various indices (Table 4) and plots are estimated and prepared using major oxides and trace elements. We corrected the estimated CaO content carbonates (calcite, dolomite) and apatite by correcting for phosphate using the measured P_2O_5 concentration [CaO* = mole CaO − mole P_2O_5 × 10/3 (Nesbitt and Young, 1982),]. When the remaining number of moles was less than that of the measured Na_2O, the CaO value was adopted as the CaO*. Otherwise, the CaO* was assumed to be equivalent to Na_2O (McLennan, 1993). The chemical index of alteration (CIA) was estimated using the expression CIA* = [Al_2O_3/(Al_2O_3 + CaO* + Na_2O + K_2O) x 100] by Nesbitt and Young (1982). The plagioclase index of alteration (PIA) was estimated from the expression PIA* = [(Al_2O_3-K_2O)/(Al_2O_3 + CaO* + Na_2O-K_2O) x 100] by Fedo et al. (1995). The index of compositional variability (ICV) was estimated as ICV = [(Fe_2O_3 + K_2O + Na_2O + CaO + MgO + TiO_2)/Al_2O_3] (wt %), (Fedo et al., 1995). Both CIA and PIA have been used widely for example as paleoclimatic indicators in the Permian of the Parana Basin, Brazil (Goldberg and Humayun, 2010), the lower Neoproterozoic strata of Aksu, Xinjiang, NW China (Ding et al., 2016), marine detrital sediments (Zhao and Zheng, 2015).

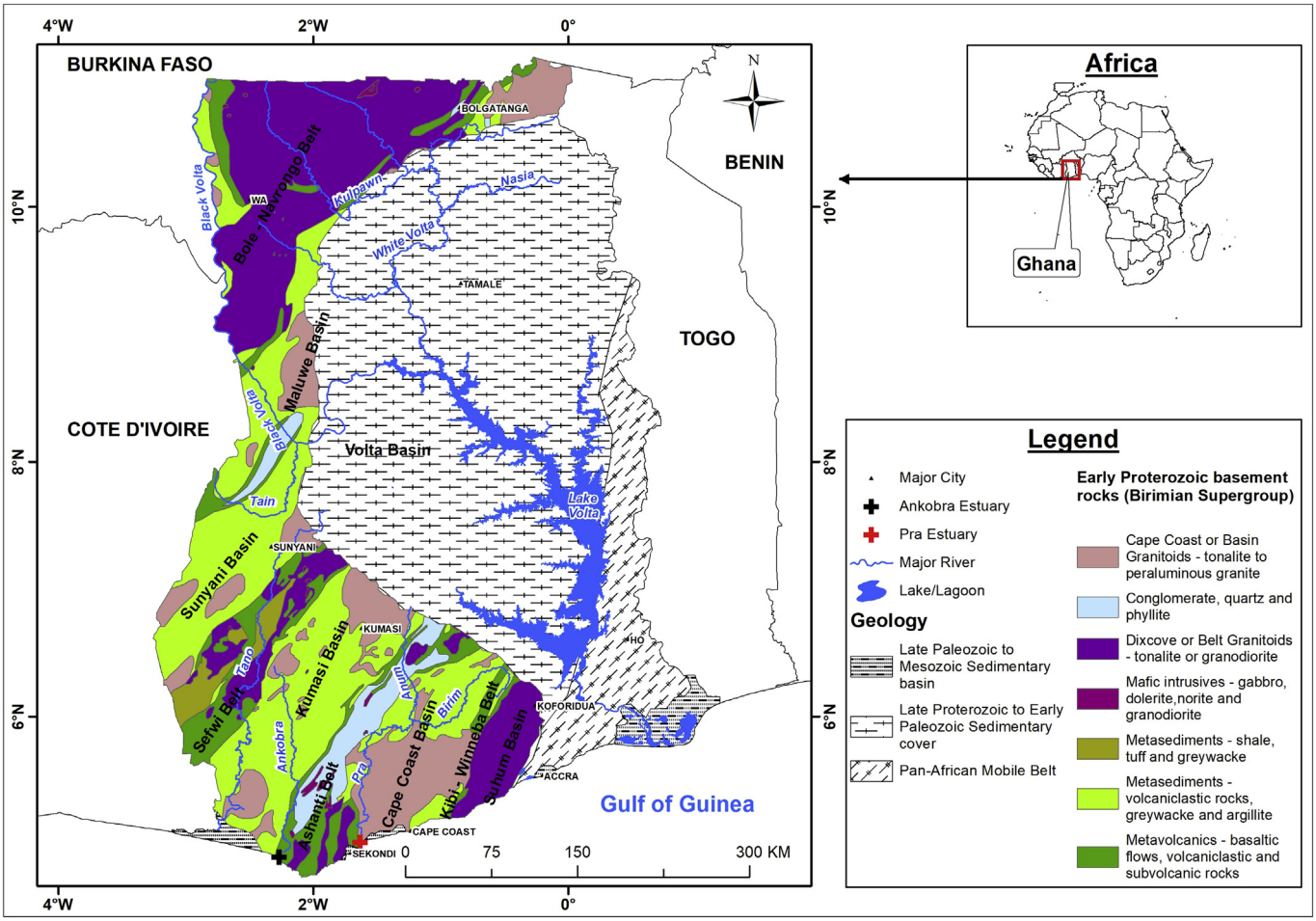

Fig. 1. Geological map showing locations of both Ankobra and Pra estuaries, basins, belts and main rock units in the Birimian Supergroup (redrawn after Peterson et al., 2018).

4. Results

4.1. Geochemistry

The geochemical compositions of the sediment cores from the Ankobra and Pra estuaries are presented in Table 2. The P_2O_5 concentrations were generally low in both estuaries with values decreasing towards recent sediments stratigraphically. Aluminum (Al_2O_3) show considerable downcore variations with values ranging from 5.3 to 14.2% in the Ankobra and 8.0–16.9% in the Pra. SiO_2 levels varied between 75.8 and 88% in the Ankobra and between 72.8 and 86.5% in the Pra. Strong linear negative trends ($r^2 > -0.82$) existed between the oxides of P, K, Al, Fe and Si in both Ankobra and Pra cores while the oxides of Ca, Na, Ti and Mg show no correlation with SiO_2 (Fig. 2). Also, the oxides of K, Fe, and P correlated positively ($r^2 > 0.80$) with Al while Ca, Ti, Na and Mg oxides showed no correlation with Al in both estuaries (Fig. 3a). Considerable variations were observed in trace element concentrations with most of the elements showing mid-core enrichment in both estuaries (Table 2). A positively strong correlation ($r^2 = 0.99$) existed between Rb and K (Fig. 3b) in both estuaries. Also, Rb, Cr, and Ni showed strong correlations ($r^2 > 0.90$) with Al in both estuaries while Mn correlated strongly with Al for only the Pra core (Fig. 3c).

4.2. Sediment characterization

Table 3 shows results of various geochemical indices used in explaining weathering and tectonic processes in the source areas of the sediments from the Pra and Ankobra estuaries. The Si/Al, Fe/K, K/Na, Al/Ti, K/Al and Na/K ratios ranged from 5.37 to 16.62, 4.47 to 6.98, 0.91 to 1.90, 12.7 to 27.35, 0.08 to 0.09 and 0.53 to 1.1 respectively in the Ankobra core. Meanwhile, the ratios of Si/Al, Fe/K, K/Na, Al/Ti, K/Al and Na/K ranged from 4.32 to 11.09, 3.67 to 5.80, 0.84 to 1.69, 13.9 to 22.22, 0.07 to 0.09 and 0.59 to 1.19 respectively in the Pra. Generally, the indices of the geochemical ratios were higher in the Ankobra core.

Using the index of chemical maturity, alkali content and the Na_2O/K_2O ratio, Pettijohn et al. (1972) proposed a classification scheme for

Table 1
Sampling information and description of ankobra and pra cores.

Estuary	Lattitude	Longitude	Water Depth (m)	Core Recovery (cm)	Color (Munsell Color Chart)
Ankobra	4.903389	−2.269278	0.8	50	Uniform Light Gray coloration throughout the whole core
Pra	5.027778	−1.6166389	0.9	52	A combination of dark gray and very dark greenish gray up to about 20 cm and then dark gray with shell from 22 cm to 40 cm

Table 2
Measured and certified mean concentrations of major oxides (% wt) and trace element (ppm DW) of standard reference material –BCSS-1.

	Major Oxides (% wt)									Trace Elements (ppm)			
	Na_2O	MgO	Al_2O_3	SiO_2	P_2O_5	K_2O	CaO	TiO_2	Fe_2O_3	V	Ni	Cr	Co
Measured Value	2.29	2.28	11.61	65.59	0.18	2.30	0.74	0.72	4.91	89.92	52.44	111.50	11.20
SE	0.06	0.04	0.18	1.43	0.01	0.06	0.01	0.01	0.11	1.55	1.04	1.96	0.06
Certified Value	2.72	2.44	11.83	66.10	0.15	2.17	0.76	0.73	4.70	93.40	55.30	123.00	11.40
SE	0.21	0.23	0.41	1.00	0.02	0.04	0.07	0.02	0.10	4.90	3.60	14.00	2.10

DW = Dry Weight.

characterizing sandstone composition based upon a plot of log (Na_2O/K_2O) vs. log (SiO_2/Al_2O_3). This scheme of classification revealed that the sediments from both estuaries were predominantly sub-arkose with few litharenites and quartz-rich (Fig. 4). The discriminant functions of Roser and Korsch (1988) used K_2O, Fe_2O_3, TiO_2, CaO, MgO, Na_2O, and Al_2O_3 compositions of sediments to distinguish among four sedimentary provenances namely: (i) Mafic Igneous provenance or P1 sediments formed in oceanic island arc; (ii) Intermediate Igneous provenance or P2 sediments formed in mature island arc; (iii) Felsic Igneous provenance or P3 sediments formed in active continental margin; and (iv) Quartzose or Recycled provenance or P4 sediments formed in passive continental margin. Plot of the source identity of the estuarine sediments using major elements in a Roser and Korsch diagram puts the sediments from both estuaries into a quartzose sedimentary or a P4 provenance region (Fig. 5a). Roser and Korsch (1986) further provided three (3) tectonic setting discriminations namely; Oceanic Island Arc (IA), Active Continental Margin (ACM) and Passive Margin (PM) using a bivariate plot of K_2O/NaO against SiO_2. This plot showed that the sediments investigated both originated from a passive margin tectonic setting (Fig. 5b).

The geochemical and mineralogical compositions of sedimentary rocks can be affected by chemical weathering (Roy et al., 2008). The intensity of chemical weathering on source materials can be deduced from bottom sediments based on the geochemical fractionation of

Table 3
Major and trace element compositions of the sediment cores from the Ankobra and Pra Estuaries.

Depth	Major oxides (wt. %)									Trace Elements (ppm)					
(cm)	Na_2O	MgO	Al_2O_3	P_2O_5	K_2O	CaO	TiO_2	Fe_2O_3	SiO_2	Mn	Rb	Sr	V	Ni	Cr	Co
Ankobra																
2.00	0.65	0.46	6.26	0.07	0.59	0.28	0.39	3.06	88.00	2.75	0.22	0.58	48.61	14.95	60.23	8.91
4.00	0.80	0.51	8.22	0.07	0.75	0.36	0.37	3.51	85.07	3.36	0.28	0.71	60.03	19.06	77.01	10.46
6.00	0.62	0.48	6.79	0.08	0.63	0.38	0.40	3.27	87.09	3.14	0.23	0.68	53.78	16.52	66.68	9.25
8.00	0.67	0.49	8.18	0.08	0.75	0.33	0.39	3.50	85.32	3.66	0.28	0.70	64.47	19.71	80.70	10.66
10.00	0.61	0.51	10.39	0.09	0.94	0.32	0.52	4.19	82.12	4.02	0.36	0.79	78.40	24.95	98.88	13.23
12.00	0.58	0.54	11.15	0.10	0.99	0.34	0.57	4.43	80.95	4.06	0.38	0.82	83.83	26.09	108.17	13.85
14.00	0.44	0.52	7.43	0.09	0.68	0.64	0.39	3.78	85.45	3.25	0.26	0.83	60.71	17.88	77.98	9.75
16.00	0.30	0.52	5.30	0.08	0.50	1.14	0.34	3.33	88.15	2.89	0.19	0.98	44.75	12.86	55.89	7.70
18.00	0.41	0.57	7.06	0.10	0.67	1.14	0.34	3.80	85.36	3.62	0.25	1.04	58.05	16.90	71.36	9.59
20.00	0.51	0.58	10.04	0.10	0.89	0.92	0.45	4.40	81.58	4.60	0.35	1.10	73.47	22.01	90.86	11.00
22.00	0.56	0.62	11.83	0.11	1.06	0.94	0.45	5.03	78.77	5.52	0.42	1.20	86.46	25.83	106.81	12.74
24.00	0.54	0.59	10.41	0.11	0.95	0.78	0.48	4.72	80.90	5.43	0.37	1.06	81.66	24.52	102.10	12.59
26.00	0.60	0.61	11.04	0.11	0.94	0.76	0.42	4.70	80.10	5.63	0.36	1.03	81.08	24.97	104.64	12.64
28.00	0.61	0.63	14.16	0.12	1.21	0.56	0.52	5.50	76.01	6.13	0.46	1.06	106.26	32.38	139.16	15.88
30.00	0.62	0.66	14.03	0.13	1.19	0.57	0.58	5.65	75.85	5.03	0.45	1.11	101.78	31.06	129.95	16.09
32.00	0.48	0.65	9.29	0.12	0.82	0.72	0.73	4.81	81.84	3.50	0.31	0.99	73.74	20.69	92.14	11.33
34.00	0.52	0.68	9.83	0.12	0.86	0.73	0.55	5.01	81.05	3.51	0.34	1.00	79.23	22.89	97.87	11.23
36.00	0.55	0.61	5.69	0.09	0.55	1.23	0.39	3.82	86.41	4.86	0.20	0.79	53.52	15.84	61.86	8.39
38.00	0.64	0.59	7.47	0.10	0.69	0.67	0.34	3.91	84.69	5.83	0.26	0.86	61.95	18.93	67.62	9.63
40.00	0.92	0.82	11.02	0.13	1.00	0.84	0.44	5.63	78.00	8.11	0.37	1.21	89.31	27.26	100.32	13.29
Pra																
2.00	0.86	0.39	8.40	0.07	0.72	0.31	0.57	2.95	85.51	2.05	0.28	0.73	53.32	17.17	58.81	10.88
4.00	0.83	0.39	8.36	0.07	0.75	0.30	0.52	2.86	85.67	2.11	0.27	0.75	54.33	17.53	60.34	12.95
6.00	0.77	0.38	8.01	0.07	0.76	0.28	0.49	2.79	86.21	2.19	0.27	0.73	52.55	16.78	57.89	12.78
8.00	0.77	0.36	7.80	0.07	0.72	0.28	0.47	2.78	86.50	2.39	0.28	0.71	52.19	16.25	57.02	12.62
10.00	0.78	0.42	10.06	0.08	0.85	0.26	0.57	3.53	83.19	2.92	0.33	0.74	69.31	21.34	75.49	15.52
12.00	0.81	0.49	12.76	0.10	1.03	0.26	0.63	4.33	79.26	3.54	0.40	0.80	86.90	27.24	94.95	17.30
14.00	0.75	0.50	13.93	0.11	1.09	0.25	0.65	4.60	77.82	3.48	0.45	0.78	94.47	29.17	103.16	17.83
16.00	0.74	0.50	13.54	0.11	1.07	0.25	0.65	4.57	78.28	3.38	0.42	0.80	90.16	27.68	97.42	17.99
18.00	0.74	0.54	12.96	0.14	0.98	0.32	0.75	5.12	77.70	3.63	0.40	0.80	86.83	27.87	94.16	17.20
20.00	0.75	0.37	9.19	0.08	0.78	0.32	0.68	3.33	84.16	2.71	0.31	0.76	60.07	18.95	65.27	12.11
22.00	0.70	0.47	11.94	0.10	0.93	0.33	0.70	4.30	79.98	3.28	0.38	0.81	77.12	25.07	84.63	16.13
24.00	0.74	0.61	16.85	0.16	1.20	0.28	0.72	5.93	72.79	4.50	0.53	0.89	113.79	35.45	123.61	22.93
26.00	0.71	0.58	15.50	0.15	1.20	0.31	0.71	5.47	74.76	4.23	0.50	0.87	107.66	33.66	117.67	21.28
28.00	0.74	0.58	15.86	0.16	1.16	0.30	0.71	5.69	74.13	4.58	0.49	0.85	108.38	33.49	117.47	20.80
30.00	0.72	0.60	16.16	0.17	1.14	0.29	0.76	5.96	73.50	4.42	0.48	0.86	110.21	34.75	118.42	21.37
32.00	0.73	0.48	11.91	0.10	0.92	0.35	0.67	4.23	80.04	3.30	0.38	0.80	80.25	25.70	89.29	16.29
34.00	0.77	0.49	11.13	0.12	0.85	0.32	0.63	4.55	80.44	3.19	0.33	0.77	73.95	24.39	79.93	15.09
36.00	0.71	0.52	11.58	0.13	0.87	0.31	0.71	4.78	79.63	3.20	0.34	0.77	76.24	25.87	81.80	15.85
38.00	0.70	0.50	10.86	0.12	0.80	0.31	0.71	4.63	80.69	3.12	0.32	0.74	72.89	24.45	79.30	15.02
40.00	0.75	0.52	10.92	0.11	0.84	0.36	0.69	4.63	80.40	3.10	0.33	0.78	72.68	24.23	78.42	16.14

Table 4
Estimated geochemical indices from the sediment cores from the ankobra and pra estuaries.

Depth (cm)	V/(V + Ni)	Ni/Co	V/Cr	CIA*	PIA*	CIW*	ICV	Si/Al	Fe/K	K/Na	Al/Ti	Na/K
Ankobra												
2.00	0.76	1.68	0.81	76.35	81.24	82.83	0.87	14.06	5.17	0.91	15.94	1.10
4.00	0.76	1.82	0.78	76.66	81.45	82.98	0.77	10.34	4.65	0.94	22.16	1.06
6.00	0.77	1.79	0.81	76.36	81.13	82.70	0.86	12.82	5.19	1.01	16.78	0.99
8.00	0.77	1.85	0.80	78.70	84.05	85.41	0.76	10.43	4.64	1.12	20.76	0.89
10.00	0.76	1.89	0.79	82.21	88.37	89.39	0.69	7.91	4.47	1.55	19.89	0.65
12.00	0.76	1.88	0.77	83.02	89.29	90.22	0.67	7.26	4.47	1.71	19.43	0.59
14.00	0.77	1.83	0.78	76.56	81.33	82.88	0.87	11.50	5.53	1.57	18.90	0.64
16.00	0.78	1.67	0.80	65.60	67.99	70.27	1.16	16.62	6.72	1.63	15.62	0.61
18.00	0.77	1.76	0.81	69.59	72.84	74.91	0.99	12.09	5.71	1.62	20.49	0.62
20.00	0.77	2.00	0.81	76.44	81.01	82.53	0.78	8.12	4.91	1.74	22.34	0.57
22.00	0.77	2.03	0.81	77.99	82.97	84.37	0.74	6.66	4.75	1.90	26.03	0.53
24.00	0.77	1.95	0.80	78.16	83.32	84.72	0.78	7.78	4.95	1.77	21.89	0.57
26.00	0.76	1.98	0.77	78.72	83.61	84.89	0.73	7.25	4.98	1.57	26.57	0.64
28.00	0.77	2.04	0.76	83.08	89.11	90.02	0.64	5.37	4.53	1.98	27.35	0.51
30.00	0.77	1.93	0.78	83.23	89.20	90.09	0.66	5.41	4.76	1.93	24.25	0.52
32.00	0.78	1.83	0.80	78.56	83.60	84.93	0.89	8.80	5.87	1.72	12.70	0.58
34.00	0.78	2.04	0.81	78.80	83.87	85.18	0.85	8.25	5.80	1.66	18.02	0.60
36.00	0.77	1.89	0.87	62.71	64.62	67.10	1.27	15.19	6.98	0.99	14.60	1.01
38.00	0.77	1.97	0.92	73.84	77.94	79.69	0.93	11.34	5.70	1.06	21.86	0.94
40.00	0.77	2.05	0.89	75.22	79.59	81.22	0.89	7.08	5.63	1.09	25.12	0.92
Pra												
2.00	0.76	1.58	0.91	77.15	81.72	83.14	0.69	10.19	4.07	0.84	14.68	1.19
4.00	0.76	1.35	0.90	77.18	81.99	83.45	0.68	10.25	3.80	0.90	15.93	1.11
6.00	0.76	1.31	0.91	77.40	82.58	84.08	0.69	10.76	3.67	0.99	16.30	1.01
8.00	0.76	1.29	0.92	77.23	82.24	83.73	0.69	11.09	3.84	0.95	16.47	1.06
10.00	0.76	1.37	0.92	81.02	86.44	87.53	0.64	8.27	4.14	1.09	17.79	0.92
12.00	0.76	1.57	0.92	83.53	89.27	90.12	0.60	6.21	4.20	1.27	20.27	0.78
14.00	0.76	1.64	0.92	85.21	91.13	91.81	0.57	5.59	4.23	1.44	21.39	0.69
16.00	0.77	1.54	0.93	85.01	90.97	91.68	0.58	5.78	4.27	1.45	20.90	0.69
18.00	0.76	1.62	0.92	84.86	90.51	91.23	0.66	5.99	5.20	1.33	17.21	0.75
20.00	0.76	1.56	0.92	79.80	84.90	86.09	0.68	9.15	4.28	1.04	13.59	0.96
22.00	0.75	1.55	0.91	83.49	89.01	89.85	0.63	6.70	4.60	1.33	17.17	0.75
24.00	0.76	1.55	0.92	87.46	93.28	93.77	0.57	4.32	4.95	1.61	23.55	0.62
26.00	0.76	1.58	0.91	86.32	92.45	93.04	0.58	4.82	4.57	1.69	21.94	0.59
28.00	0.76	1.61	0.92	86.83	92.73	93.26	0.58	4.67	4.89	1.58	22.22	0.63
30.00	0.76	1.63	0.93	87.64	93.43	93.90	0.59	4.55	5.24	1.58	21.16	0.63
32.00	0.76	1.58	0.90	83.02	88.37	89.24	0.62	6.72	4.58	1.26	17.87	0.79
34.00	0.75	1.62	0.93	82.76	87.97	88.85	0.69	7.23	5.35	1.10	17.53	0.91
36.00	0.75	1.63	0.93	84.11	89.48	90.25	0.69	6.88	5.52	1.21	16.31	0.82
38.00	0.75	1.63	0.92	83.74	88.92	89.71	0.71	7.43	5.80	1.14	15.38	0.88
40.00	0.75	1.50	0.93	82.24	87.34	88.27	0.72	7.36	5.53	1.11	15.88	0.90

mobile and immobile cations during weathering (Nesbitt and Young, 1982). The estimated CIA, PIA and CIW indices were above 70 (Table 3). The A–CN–K diagram clearly shows a silicate weathering trend of both the Ankobra and Pra sediments (Fig. 6a). A strongly negative linear relationship ($r^2 = -0.81$) existed between the CIA and ICV with very high CIA values corresponding to low ICV values (Fig. 7a). The CIA values particularly of the sediments from the Pra estuary are related linearly with Al/Na, Ti/Na but not K/Na (Fig. 7b, c and 7d).

The extent of chemical weathering of geologic materials is a consequence of climate as well as rates of tectonic uplift and exposure (Wronkiewicz and Condie, 1987). The SiO_2 vs. ($Al_2O_3 + K_2O + Na_2O$) (after Suttner and Dutta, 1986) indicates that the weathered sediments in their source regions have been exposed predominantly to semi-humid to semi-arid climatic conditions (Fig. 8).

Knowledge about paleo-redox conditions is necessary for reconstructing and understanding how oxygenation processes of primary production and respiration in both environments has affected DO_2 levels in both estuaries through time. The ratios of V/(V + Ni) V/Cr and Ni/Co were less than 0.8, 2 and 5 (Table 3).

5. Discussions

5.1. Chemical mobility/immobility effects of elements in sediments

To understand the changes in chemical processes that occurred in the sediments during the processes of erosion, transportation and after deposition, it is necessary to evaluate the chemical mobility/immobility of the analyzed elements in the sediment samples. This helps in distinguishing changes due to physical process of sorting from those due to chemical weathering. The graphical method proposed by Fralick and Kronberg (1997) allows identification of immobile elements in a given sediment sample through the use of binary diagrams. This method is based on the principle that plots of pair of immobile elements hosted in sediments from a common source, having similar hydrodynamic behavior will form a linear array of coordinates on binary diagrams. Any substantial deviation from the above trend may imply either selective chemical fractionation or multiplicity of source to the sediments. The strong positive correlations of P, Fe, Rb, Cr, Ni with Al in both estuaries suggests that these elements were chemically immobile and hydraulically fractionated. Mn trend observed suggests a chemical fractionation of the element in the Ankobra and hydraulic sorting of the element in the Pra. Slingerland and Smith (1986) described four hydraulic sorting mechanisms of elements based on appropriate tectonic and geomorphic setting. These mechanisms are: suspension sorting which operates during deposition; entrainment sorting which operates

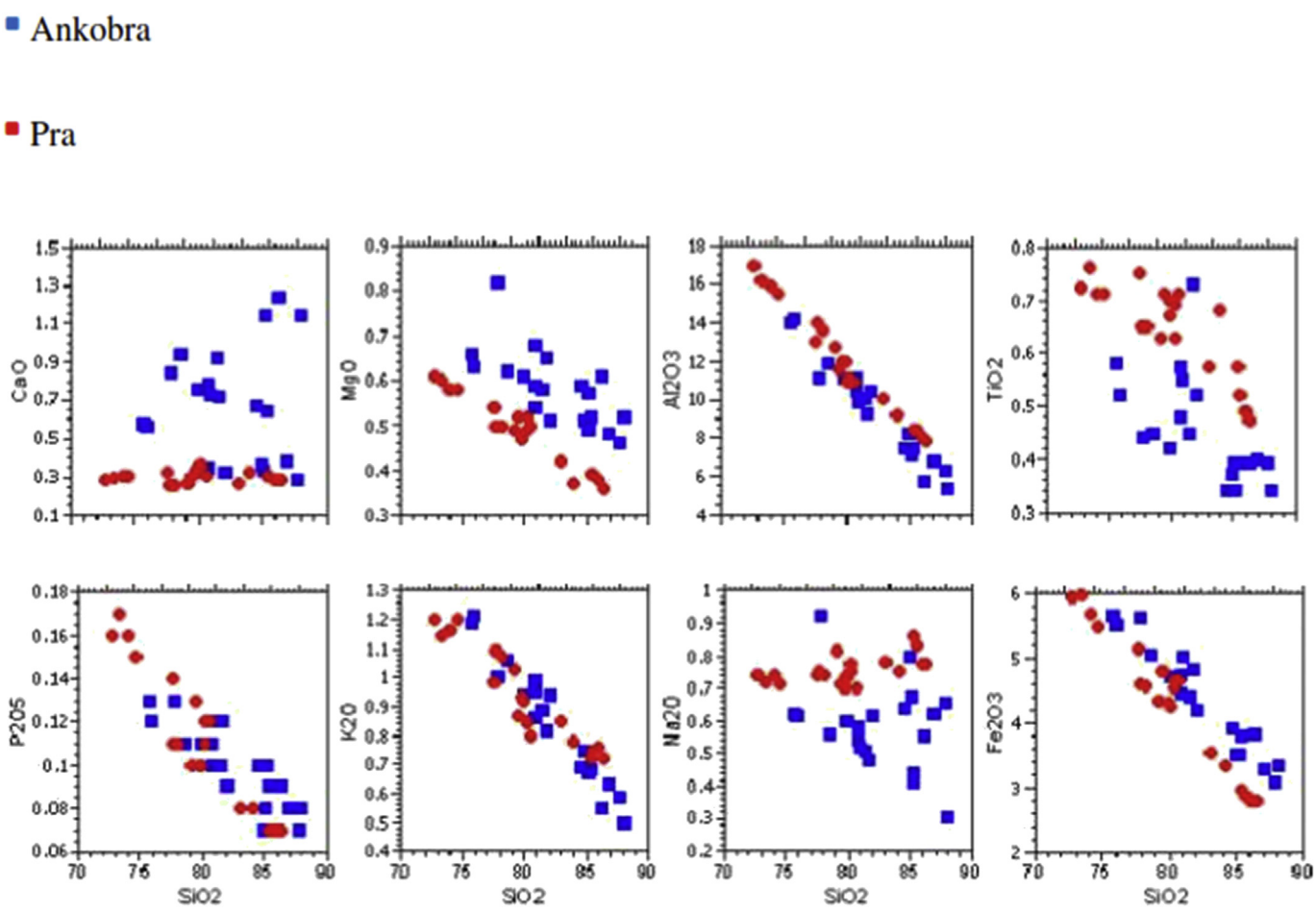

Fig. 2. Harker major element variation (in wt %) diagrams for the investigated sediments from the Ankobra (shaded squares) and Pra (shaded circles) estuaries showing plots of SiO_2 vs different oxides.

during erosion; and transport and shear sorting which operates during transportation. The nature of the sediment grains from both estuaries suggests that the elements could have separated during deposition in the estuaries although other sorting mechanisms could have occurred during transport as well. The weaker trends observed in plots of Na, Ti, Ca and Mg against Al may be attributed to selective chemical fractionation that occurred in the sediment matrix or their source rocks during transportation, deposition and post-deposition (Fralick and Kronberg, 1997; Singh, 2009). The strong correlation coefficient between Al_2O_3 and K_2O ($r^2 = 0.95$) as opposed to Al_2O_3 and CaO in the sediments from both the Ankobra and Pra suggests *k*-feldspar control on the major element composition (Hossain et al., 2014). This is also supported by the positive correlation between K_2O and Rb. The plots of elements against SiO_2 provide further insight into chemical mobility of the elements and hydrodynamic behavior of their major mineral phases (Fralick and Kronberg, 1997). SiO_2 against immobile element plots will result in a linear arrangement of points extending either towards 0% (if major mineral phases containing the elements are concentrated in the sand) or 100% (for elements concentrated in fine fraction) (Fralick and Kronberg, 1997). The negative trend observed in the P, K, Al, Fe against SiO_2 also confirms their chemically immobile nature and suggests that the mineral phases containing the elements are concentrated from the fine fraction. Since P, K, Al and Fe are immobile and show hydrodynamic similarity of the mineral phases holding them; their ratio should be same as the average ratio of these elements in their source (Singh, 2009).

5.2. Provenance, tectonic setting and source area weathering

The geochemical signatures of the Ankobra and Pra estuary sediments have been used to unravel various provenance characteristics. Cox et al. (1995) used the ratio of K/Al to differentiate between sediments rich in either feldspar or clay minerals. According to their scheme, sediments with K/Al ratios ranging from 0.3 to 0.9 are enriched in feldspars while those with K/Al ratios ranging from 0.0 to 0.3 are concentrated with clay minerals (Cox et al., 1995). The very low values of K/Al values obtained in both cores from this study therefore suggests the predominance of clay minerals relative to k-feldspar minerals in the sediments from the two estuaries. The ratio of SiO_2/Al_2O_3 in both sediments shows low level of feldspar as compared to quartz content, thereby implying that, the sediments are quite compositionally matured. This level of maturity is further confirmed by the low Na_2O/K_2O ratios (Roser and Korsch, 1986). The plot of log (Na_2O/K_2O) vs. log (SiO_2/Al_2O_3) revealed the investigated sediments from both estuaries were mostly sub-arkosic with few litharenites, suggesting a sub-mature to mature type of sediments.

The Al_2O_3/TiO_2 ratios of rocks and sediments are essentially used to infer the source-rock compositions. Hayashi et al. (1997) showed Al_2O_3/TiO_2 ratios from 21 to 70, 8 to 21 and 3 to 8 to be felsic igneous, intermediate and mafic igneous rocks respectively. The values obtained in this study for both estuaries indicate that the sediments were derived from a mixture of intermediate to mafic igneous rocks. The discriminant functions of Roser and Korsch (1988) revealed the sediments originated from a quartzose provenance region formed in a passive continental margin. This result suggests that sediments from both the Ankobra and

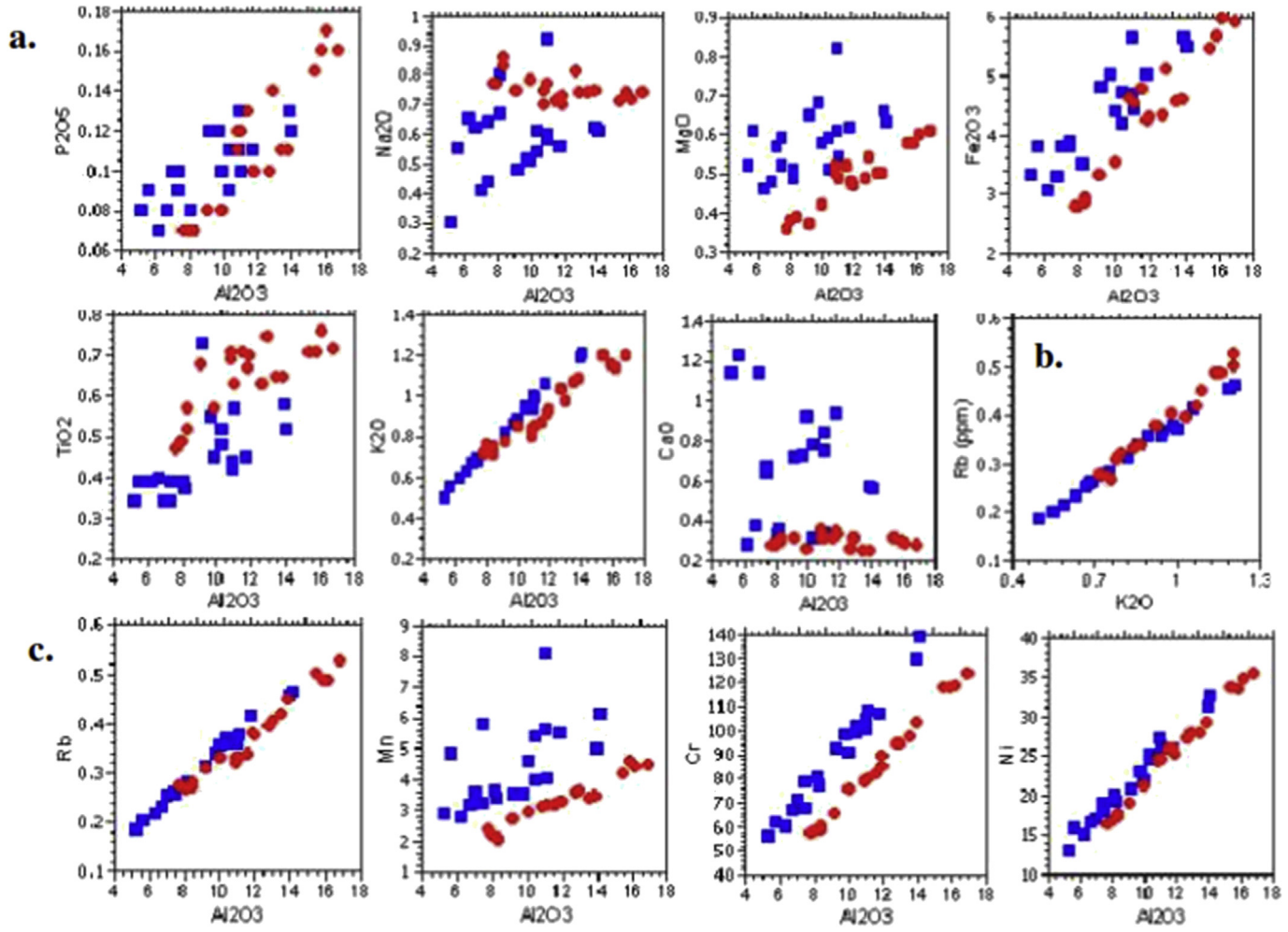

Fig. 3. Harker variation diagrams for the investigated sediments from the Ankobra (shaded squares) and Pra (shaded circles) estuaries showing plots of: (a) Al_2O_3 (in wt%) vs. different oxides (in wt%); (b) Rb vs. K_2O and (c) Al_2O_3 (in wt%) vs trace elements (in ppm).

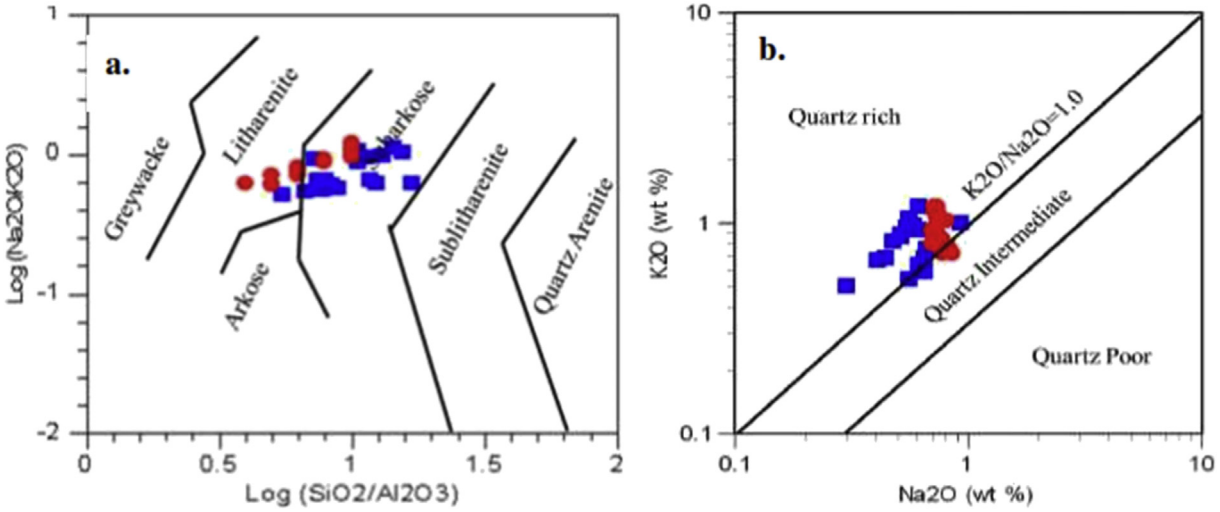

Fig. 4. Plot of the investigated estuarine sediments from the Ankobra (shaded squares) and Pra (shaded circles) on geochemical classification diagrams; (a) log (Na_2O/K_2O) vs. log (SiO_2/Al_2O_3) (after Pettijohn et al., 1972) and (b) Plot of Na_2O versus K_2O (after Crook, 1974).

Pra have probably undergone intense hydraulic and geochemical fractionation. The typical rock composition of the underlying rocks of both rivers as indicated earlier are generally dacitic volcaniclastics, wackes and argillitic sediments as well as granitoids (Fig. 1; Petersson et al., 2018; Leube et al., 1990). The make-up of these underlying rocks suggests the resultant sub-arkosic nature of sediments obtained possibly from the granitoids and the subsequent overall quartzose signatures of the sediments possibly contributed from the argillitic sediments with

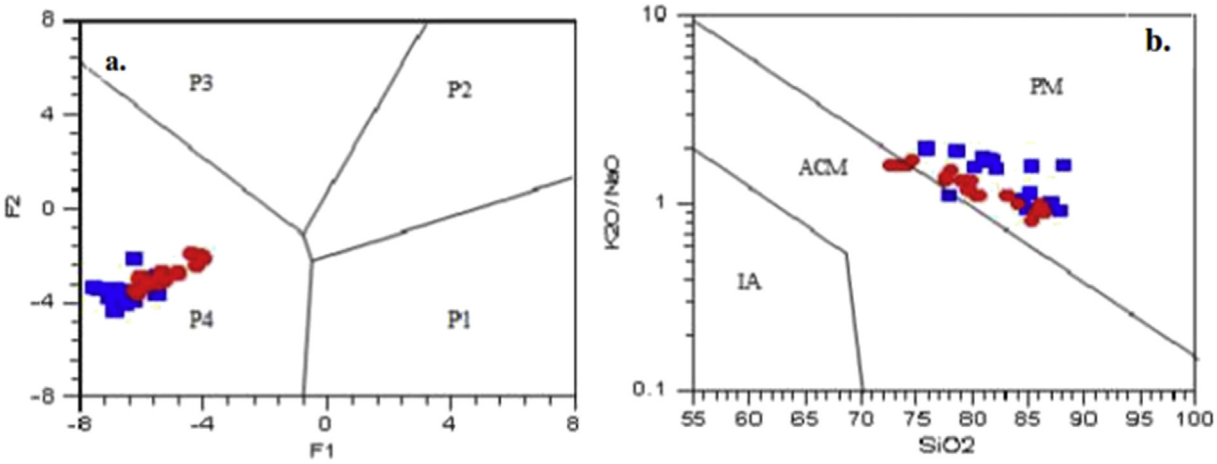

Fig. 5. (a) Discriminant function plots showing the source of the sediment samples from the Ankobra (shaded square) and Pra (shaded circle) estuaries using major elements (after Roser and Korsch, 1988). (b) Tectonic setting discrimination diagram of SiO_2 vs. log (K_2O/Na_2O) for the investigated Holocene sediments (after Roser and Korsch, 1986).

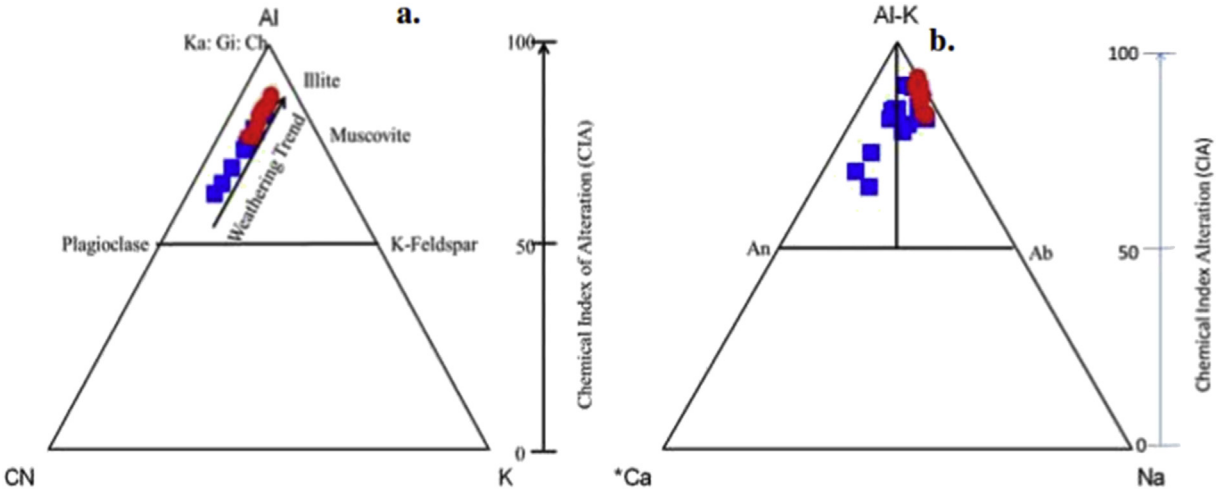

Fig. 6. A-CN-K, (Al-K)-Ca*-Na ternary diagrams of sediments from the Ankobra (shaded squares) and Pra (shaded circles) estuaries.

the intermediate and mafic content of sediments from the dacitic volcaniclastics.

Sediments in aquatic systems form through weathering and the transport of weathered materials either fluvially or via wind. Weathering affects the geochemistry and mineralogy of sediments deposited in aquatic ecosystems and explains any geochemical transformation in mineralogy that occurred during the transport process. The high CIA, PIA and CIW values obtained at all sections of the cores from both estuaries depict moderate to extreme chemical weathering of the grains at source and also during transport (Cox et al., 1995; Fedo et al., 1995). Also the CIA estimations are compatible with the PIA values suggesting the sediments have undergone high plagioclase rather than K-feldspar weathering. With increasing CIA and PIA values, the sediments are depleted in Na_2O and *CaO relative to K_2O but enriched in Al_2O_3. This was very evident in the A–CN–K diagram where clear trends of hydrolytic/silicate weathering were observed in both the Ankobra and Pra sediments. While hydrolytic weathering may affect the chemical composition of the sediments, it is also important to note that transport sorting could also exert a major influence on the composition of the sediments. Along a river and transport path, labile mineral grains will be leached preferentially. A combination of transport sorting and chemical weathering will lead to labile grains such as feldspar becoming prone to progressive decay along cleavages, cracks and other zones of lattice weakness. This decay will result in eventual transformation of feldspars into clay minerals, and a compositionally matured sediment deposits formed (Johnsson et al., 1988). The ICV of the studied estuarine sediments are less than 1 in most cases suggesting that they are compositionally mature and were likely dominated by second cycle or recycled inputs (Cullers and Podkovyrov, 2000). The sediments from both estuaries plotted parallel to the A–CN line, suggesting that they have similar compositions of unweathered parent materials. The trend of weathering of plagioclase of the estuarine sediments shows a linear plot and therefore, suggests that the probable provenance consists of plagioclases which are slightly enriched in anorthite (Roy et al., 2008). As PIA estimates increase however, the samples, particularly those from the Pra exhibit values that are low in CaO* and plot near the Al_2O_3 apex of the triangle. This indicates that as the chemical weathering increases the sediments are enriched in secondary aluminous clay minerals and gradually depleted in anorthite (Roy et al., 2008). Again considering that, Veizer and Jansen (1979) estimated on a global basis that clastic sediments are 65% recycled, one can say that the sediments from both estuaries are recycled and this is in line with the provenance classification which categorized the sediments as P4 or recycled. A low CIA and high ICV showing very little proof of weathering, suggest they are likely to originate from young igneous rocks, however, a high CIA and low ICV is attributed to either intense weathering of the source material or recycling of previously weathered material.

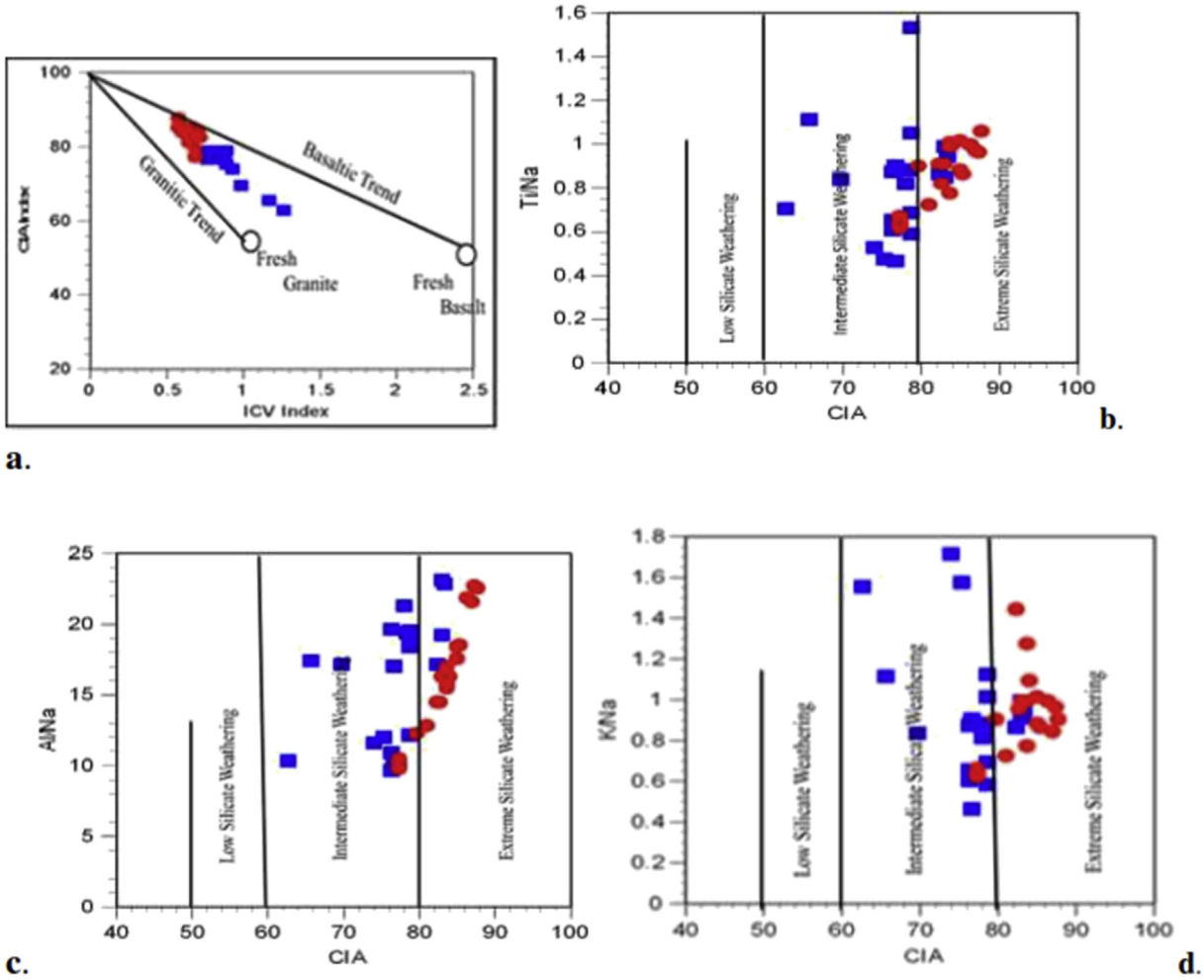

Fig. 7. Scatter plots of chemical index of alteration (CIA) vs. index of compositional variability (ICV), Al/Na, Ti/Na, and K/Na in the sediments from the Ankobra (shaded squares) and Pra (shaded circles) estuaries.

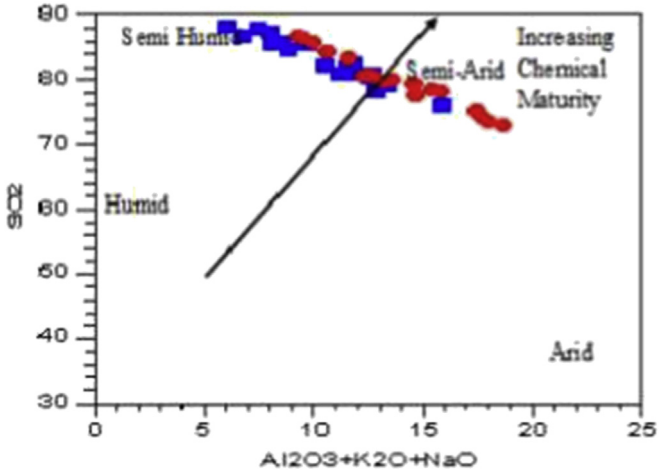

Fig. 8. Bivariate plot of SiO_2 (% wt) vs. (Al2O3 + K2O + Na2O) to discriminate paleoclimatic condition during the deposition of the Ankobra (shaded squares) and Pra (shaded circles) estuarine sediments (after Suttner and Dutta, 1986).

5.3. Paleo-climate of source material and paleo-redox conditions of the estuaries

The extent of chemical weathering of a parent rock is a consequence of climate as well as rates of tectonic uplift and exposure (Wronkiewicz and Condie, 1987). A high CIA value indicates a shift in climatic regime towards warm and humid conditions and/or decrease in tectonic activity favored chemical weathering in the source regions (Moosavirad et al., 2012). The high CIA, PIA, CIW values estimated and low ICV values of the sediments reflect intense weathering of source rocks and points to warm and humid climate conditions. This agrees with SiO_2 vs. ($Al_2O_3 + K_2O + Na_2O$) plot of Suttner and Dutta (1986) which puts sediments as originating from sources in two regimes of semi-arid to semi-humid climatic conditions.

Redox conditions, generally indicated as molecular oxygen relative to dissolved sulfide, are constrained by biological processes, volcanic emissions, weathering reactions as well as mixing in aquatic environments (Severmann and Anbar, 2009). Paleo-redox reconstructions are especially appropriate because O_2 which is produced by photosynthesis, and respiration which consumes O_2, brings about a close relationship between oxygenation and the carbon cycle. As such redox condition indicators may indicate a change in the carbon cycle which may be as a result of excessive nutrients input giving rise to eutrophication or vice versa. The degree of how soluble vanadium is in natural waters, its adsorption onto suspended particles in the water column and deposition in the bottom are largely affected by redox conditions (Bellanca et al., 1996). For example, in the Black sea, dissolved V concentrations are depleted by approximately 60% in reducing deep waters, suggesting that reducing sediment may serve as a major sink for V (Nameroff et al., 2002). Vanadium is enriched mostly in reducing environments, where

the reduction of sulphate is more effective (Hossain et al., 2014). Nickel on the other hand is mostly enriched in organic-rich sediments (Gilkson et al., 1985). The proportionality of these two elements V/(V + Ni) is therefore important in determining the physicochemical conditions (redox potential (Eh), the concentration of hydrogen ions (pH) and the activity of sulfide ions) controlling the formation of organometallic compounds, such as (Hossain et al., 2014; Madhavaraju and Lee, 2009; Galarraga et al., 2008). Additionally, the V/Cr ratio has been adopted as an indicator of paleo-oxygenation by several authors (Dill, 1986; Dill et al., 1988). Chromium is largely integrated in the detrital components of sediments which may be a replacement for Al in the clay framework and V is mostly established among sediments in reducing environments (Shaw et al., 1990). Ratios above 2 suggest anoxic conditions, whiles values below 2 indicate more oxidizing conditions (Jones and Manning, 1994). Most sections of the core from the Ankobra estuary and all sections from the Pra estuary had V/Cr below 2 suggesting the sediments were deposited under oxic conditions. This oxic depositional environment is further confirmed by the Ni/Co ratios which were below 5 for all the sediments from both estuaries. Ni/Co ratios below 5 signify oxic environments, while those above 5 connote suboxic and anoxic environments (Jones and Manning, 1994). Contrary to the V/Cr and Ni/Co ratios, the V/(V + Ni) ratios for both estuaries ranged between 0.75 and 0.78 depicting anoxic depositional conditions. This dissimilarity in results between different redox trace-element ratios has also been observed by Rimmer (2004). It is therefore suggested that absolute thresholds established in other studies should be applied carefully, however, ratios may provide information on relative differences in redox conditions (Rimmer, 2004).

6. Conclusions

Sediments play a key role in defining and elucidating the geochemistry and geology of source regions. Their chemical compositions are shaped by factors such as source rock geochemistry, climate, chemical weathering and sorting processes during transportation, deposition and diagenesis. The sediments from both the Ankobra and Pra estuaries exhibited similar downcore trends in their major element and trace element geochemistry suggesting similarities in their source rock compositions.

The investigated sediments from both estuaries predominantly compose of sub-arkoses with few litharenites. Some major oxides and trace elements correlate positively with Al_2O_3 thereby confirming clear hydraulic fractionation.

Estimated Al_2O_3/TiO_2 ratio indicated some intermediate to felsic granitoid source rocks. The provenance and tectonic discrimination diagrams suggests quartzose rocks formed in a passive continental margin in upstream regions of the Ankobra and Pra estuaries. Thus, suggesting a probable multiple sediment supply source for both estuaries.

The estimated CIA, PIA and CIW indices were above 70 at all sections of the cores from both estuaries depicting moderate to extreme weathering of the source materials resulting in low ICVs. Also the CIA values were consistent with the PIA values suggesting the sediments have undergone high plagioclase relative to K-feldspar weathering. Although the sediments from both estuaries were deposited under semi-arid to semi-humid conditions, the CIA and PIA values depict warm and humid climatic conditions in their source regions. Paleo-redox analysis of the cores suggests the Holocene sediments from both estuaries were deposited under oxic deltaic conditions.

Acknowledgements

We wish to thank the International Foundation for Science (grant # W 5331-1) and the International Students Exchange Program (ISEP) for their immense contributions towards the project. We are grateful to Mr. Mario Boateng and Mr. Emmanuel Klubi both of the Department of Marine and Fisheries Sciences of the University of Ghana for their roles in sample collection and preparations.

References

Azcue, J.M., Nriagu, J.O., 1995. Impact of abandoned mine tailings on the arsenic concentrations in Moira Lake, Ontario. J. Geochem. Explor. 52, 81–89.
Bellanca, A., Claps, M., Erba, E., Masetti, D., Neri, R., Premolisilva, I., Venezia, F., 1996. Orbitally induced limestone/marlstone rhythms in the Albian-Cenomanian Cismon section (Venetian region, northern Italy): sedimentology, calcareous and siliceous plankton distribution, elemental and isotope geochemistry. Paleogeogr. Paleoclimatol. Paleoecol. 126, 227–260.
Burgos, M., Rainbow, P., 2001. Availability of cadmium and zinc from sewage sludge to the flounder, Platichthys flesus, via a marine food chain. Mar. Environ. Res. 51, 417–439.
Condie, K.C., 1993. Chemical Composition and Evolution of the Upper Continental Crust; Contrasting Results from Surface Samples and Shales. Chem. Geol. 104, 1–37. https://doi.org/10.1016/0009-2541(93)90140-E.
Cox, R., Low, D.R., Cullers, R.L., 1995. The influence of sediment recycling and basement composition on evolution of mudrock chemistry in the southwestern United States. Geochem. Cosmochim. Acta 59, 2919–2940.
Crook, K.A.W., 1974. Lithogenesis and Geotectonics: The Significance of Compositional Variation in Flysch Arenites (Greywackes), vol. 19. SEPM, Special Publication, pp. 304–310.
Cullers, R.L., 2002. Implications of elemental concentrations for provenanace, redox conditions, and metamorphic studies of shales and limestones near Pueblo, Co, USA. Chem. Geol. 191, 305–327.
Cullers, R.L., Podkovyrov, V.N., 2000. Geochemistry of the Mesoproterozoic Lakhanda shales in southeastern Yakutia, Russia: implications for mineralogical and provenance control, and recycling. Precambrian Res. 104, 77–93.
Dill, H., 1986. Metallogenesis of early paleozoic graptolite shales from the graefenthal horst (northern Bavaria-Federal Republic of Germany). Econ. Geol. 81, 889–903.
Dill, H., Teshner, M., Wehner, H., 1988. Petrography, inorganic and organic geochemistry of Lower Permian Carboniferous fan sequences (Brandschiefer Series) FRG: constraints to their palaeogeography and assessment of their source rock potential. Chem. Geol. 67 (3–4), 307–325.
Ding, H., Ma, D., Yao, C., Lin, Q., Jing, L., 2016. Implication of the chemical index of alteration as a paleoclimatic perturbation indicator: an example from the lower Neoproterozoic strata of Aksu, Xinjiang, NW China. Geosci. J. 20 (1), 13–26.
Dobrzinski, N., Bahlburg, H., Strauss, H., Zhang, Q.R., 2004. Geochemical climate proxies applied to the Neoproterozoic glacial succession on the Yangtze Platform, South China. In: Jenkins, G., Mc Memenamin, M., Mackay, C.P., Sohl, L. (Eds.), The Extreme Proterozoic: Geology, Geochemistry and Climate. American Geophysical Union Monograph Series. vol. 146. pp. 13–32.
Ehrlich, H.L., 1996. Geomicrobiology, third ed. Marcel Dekker, New York, pp. 719.
Fedo, C.M., Nesbitt, H.W., Young, G.M., 1995. Unraveling the effects of potassium metasomatism in sedimentary rocks and paleosols, with implications for paleoweathering conditions and provenance. Geology 23, 921–924.
Fralick, W., Kronberg, B.I., 1997. Geochemical discrimination of elastic sedimentary rock source. Sediment. Geol. 113, 111–124.
Galarraga, F., Reategui, K., Martinez, A., Martinez, M., Llamas, J.F.L., Marquez, G., 2008. V/Ni ratio as a parameter in palaeoenvironmental characterisation of nonmature medium-crude oils from several Latin American basins. J. Petrol. Sci. Eng. 61 (1), 9–14.
Gilkson, M., Chappell, B.W., Freeman, R.S., Webber, E., 1985. Trace elements in oil shales, their source and organic association with particular reference to Australian deposits. Chem. Geol. 53, 155–174.
Goldberg, K., Humayun, M., 2010. The applicability of the chemical index of alteration as a paleoclimatic indicator: an example from the permian of the Parana Basin, Brazil. Palaeogeogr. Palaeoclimatol. Palaeoecol. 293, 175–183.
Hayashi, K., Fujisawa, H., Holland, H.D., Ohomoto, H., 1997. Geochemistry of ~1.9 Ga sedimentary rocks from northeastern Labrador, Canada. Geochem. Cosmochim. Acta 61, 4115–4137.
Hossain, I., Roy, K.K., Biswas, P.K., Alam, M., Moniruzzaman, Md, Deeba, F., 2014. Geochemical characteristics of Holocene sediments from Chuadanga district, Bangladesh: implications for weathering, climate, redox conditions, provenance and tectonic setting. Chin. J. Geochem. 33, 336–350.
Jacobson, A.D., Blum, J.D., Chamberlian, C.P., Craw, D., Koons, P.O., 2003. Climate and tectonic controls on chemical weathering in the New Zealand Southern Alps. Geochem. Cosmochim. Acta 37, 29–46.
Johnsson, M.J., Stallard, R.F., Meade, R.H., 1988. First-cycle quartz arenites in the orinoco river basin, Venezuela and Colombia. J. Geol. 96, 263–277.
Jones, B., Manning, D.C., 1994. Comparison of geochemical indices used for the interpretation of paleo-redox conditions in ancient mudstones. Chem. Geol. 111, 111–129.
Leube, A., Hirdes, W., Mauer, R., Kesse, G., 1990. The early proterozoic birimian supergroup of Ghana and some aspects of its associated gold mineralization. Precambrian Res. 46, 139–165.
Madhavaraju, J., Lee, Y.I.I., 2009. Geochemistry of the dalmiapuram formation of the uttatur Group (early creataceous), cauvery basin, southeastern India: implications on provenance and paleo-redox conditions. Rev. Mex. Ciencias Geol. 26 (2), 380–398.
Mahu, E., 2014. Geochemistry of Estuarine Sediments of Ghana: Provenance, Trace Metal Accumulation Trends and Ecotoxicological Risks. A PhD Thesis Submitted to the Department of Marine and Fisheries Sciences. University of Ghana.
Mahu, E., Nyarko, E., Hulme, S., Coale, K.H., 2015. Distribution and enrichment of trace

metals in marine sediments from the eastern equatorial atlantic, off the coast of Ghana in the Gulf of Guinea. Mar. Pollut. Bull. 98, 301–307.
Mahu, E., Nyarko, E., Hulme, S., Swarzenskic, P., Asiedu, D., Coale, K., 2016. Geochronology and historical deposition of trace metals in three tropical estuaries in the Gulf of Guinea. Estuar. Coastal Shelf Sci. 177, 31–40.
McLennan, S.M., 1993. Weathering and global denudation. J. Geol. 101, 295–303.
Moosavirad, S.M., Janardhana, M.R., Sethumadhav, M.S., Narasimha, K.N.P., 2012. Geochemistry of lower jurassic sandstones of shemshak formation, kerman basin, Central Iran: provenance, source weathering and tectonic setting. J. Geol. Soc. India 79, 483–496.
Morillo, J., Usero, J., Rojas, R., 2008. Fractionation of metals and as in sediment from a biosphere reserve (Odiel salt marshes) affected by acidic mine drainage. Environ. Monit. Assess. 139, 329–337.
Mortazavi, M., Moussavi-Harami, R., Mahboubi, A., 2014. Geochemistry of the late jurassic–early cretaceous shales (shurijeh formation) in the intracontinental kopet-dagh basin, northeastern Iran: implication for provenance, source weathering, and paleoenvironments. Arab Journal of Geoscience 7, 5353–5366.
Nameroff, T.J., Balistrieri, L.S., Murray, J.W., 2002. Suboxic trace metal geochemistry in the eastern tropical North Pacific. Geochem. Cosmochim. Acta 66, 1139–1158.
Nesbitt, H.W., Young, G.M., 1982. Early Proterozoic climates and plate motions inferred from major element chemistry of Lutites. Nature 299, 715–717.
Nesbitt, H.W., Young, G.M., 1996. Petrogenesis of sediment in the absence of chemical weathering: effects of abrasion and sorting on bulk composition and mineralogy. Sedimentology 43, 341–358.
Osae, S., Asiedu, D.K., Yakubo, B., Koeberl, C., Dampare, S.B., 2006. Provenance and tectonic setting of Late Proterozoic Buem sandstones of southeastern Ghana: evidence from geochemistry and detrital modes. J. Afr. Earth Sci. 44, 85–96.
Petersson, A., Scherstén, A., Gerdes, A., 2018. Extensive reworking of Archaean crust within the Birimian terrane in Ghana as revealed by combined zircon U-Pb and Lu-Hf isotopes. Geosci. Frontiers 9, 173–189. https://doi.org/10.1016/j.gsf.2017.02.006.
Pettijohn, F.J., Potter, P.E., Siever, R., 1972. Sand and Sandstone. Plate motions inferred from major element chemistry of lutites. Precambrian Res. 147, 124–147.
Ridgway, J., Shimmield, G., 2002. Estuaries as repositories of historical contamination and their impact on shelf seas. Estuar. Coastal Shelf Sci. 55, 903–928.
Rimmer, S.M., 2004. Geochemical paleoredox indicators in the devonian-mississipian Black shales, central appalachian basin, USA. Chem. Geol. 206, 373–391.
Roser, B.P., Korsch, R.J., 1986. Determination of tectonic setting of sandstones and mudstones suites using SiO_2 content and K_2O/Na_2O ratio. J. Geol. 94, 635–650.
Roser, B.P., Korsch, R.J., 1988. Provenance signature of sandstone-mudstone suite determined using discriminant function analysis of major element data. Chem. Geol. 67, 119–139.
Roy, P.D., Caballero, M., Lozano, R., Smykatz-Kloss, W., 2008. Geochemistry of Late Quaternary sediments from Tecocomulco lake, central Mexico: implication to chemical weathering and provenance. Chemie der Erde-Geochem. 68, 383–393.
Severmann, S., Anbar, D.A., 2009. Reconstructing paleoredox conditions through a multitracer approach: the key to the past is the present. Elements 5, 359–364.
Shaw, T.J., Geiskes, J.M., Jahnke, R.A., 1990. Early diagenesis in differing depositional environments: the response of transition metals in pore water. Geochem. Cosmochim. Acta 54, 1233–1246.
Singh, P., 2009. Major, trace and REE geochemistry of the Ganga River sediments: influence of provenance and sedimentary processes. Chem. Geol. 266, 242–255.
Singh, P., Rajamani, V., 2001. REE geochemistry of recent clastic sediment from the Kaveri floodplains, southern India: implications to source weathering and sedimentary processes. Geochem. Cosmochim. Acta 65, 3093–3108.
Slingerland, R., Smith, N.D., 1986. Occurrence and Formation of Water-laid Placers: Annual Review of Earth and Planetary Sciences. vol. 14. pp. 113–147.
Suttner, L.J., Dutta, P.K., 1986. Alluvial sandstone composition and paleoclimate 1. Framework mineralogy. J. Sediment. Petrol. 56, 326–345.
Veizer, J., Jansen, S.L., 1979. Basement and sedimentary recycling and continental evolution. J. Geol. 87, 341–370.
Weltje, G.J., von Eynatten, H., 2004. Quantitative provenance analysis of sediment: review and outlook. Sediment. Geol. 171, 1–11.
Wronkiewicz, D.J., Condie, K.C., 1987. Geochemistry of archean shales from the witwatersrand supergroup, South Africa: source-area weathering and provenance. Geochem. Cosmochim. Acta 51, 2401–2416.
Zhao, M.Y., Zheng, Y.F., 2015. The intensity of chemical weathering: geochemical constraints from marine detrital sediments of Triassic age in South China. Chem. Geol. 391, 111–122.